RESEARCH PAPER

Acta Neurobiol Exp 2021, 81: 233–248
DOI: 10.21307/ane-2021-022

Inhibition of ionotropic GluR signaling preserves oligodendrocyte lineage and myelination in an *ex vivo* rat model of white matter ischemic injury

Mohamed A. Al-Griw[1]*, Michael G. Salter[2] and Ian C. Wood[3]

[1] *Department of Histology and Genetics, Faculty of Medicine, University of Tripoli, Tripoli, Libya,*
[2] *Thornton-le-Moor, North Yorkshire, United Kingdom,*
[3] *Faculty of Biological Sciences, University of Leeds, Leeds, United Kingdom,*
** Email: m.algriw@uot.edu.ly*

Preterm infants have a high risk of neonatal white matter injury (WMI). WMI leads to reduced myelination, inflammation, and clinical neurodevelopmental deficits for which there are no effective treatments. Ionotropic glutamate receptor (iGluR) induced excitotoxicity contributes to oligodendrocyte (OL) lineage cell loss and demyelination in brain models of neonatal and adult WMI. Here, we hypothesized that simulated ischemia (oxygen-glucose deprivation) damages white matter *via* activation of iGluR signaling, and that iGluR inhibition shortly after WMI could mitigate OL loss, enhance myelination, and suppress inflammation in an *ex vivo* cerebellar slice model of developing WMI. Inhibition of iGluR signaling by a combined block of AMPA and NMDA receptors, shortly after simulated ischemia, restored myelination, reduced apoptotic OLs, and enhanced OL precursor cell proliferation and maturation as well as upregulated expression of transcription factors regulating OL development and remyelination. Our findings demonstrate that iGluR inhibition post-injury alleviates OL lineage cell loss and inflammation and promotes myelination upon developing WMI. The findings may help to develop therapeutic interventions for the WMI treatment.

Key words: neonatal white matter injury, ischemia, ionotropic glutamate receptors, oligodendrocytes, oligodendrocyte precursors

INTRODUCTION

Increasing evidence suggest that there are many factors potentially involved in the impaired brain development in preterm infants (Ogawa et al., 2020). Among these is the excitotoxic injury (Salter and Fern, 2005; Fern and Matute, 2019; Ogawa et al., 2020). All these disturbances could lead to impaired oligodendrocyte (OL) maturation, cell death, a loss of appropriate myelination, and eventually – development of the condition named "white matter injury (WMI)" and neurological disorders. Since oligodendrogenesis and myelination takes place during the third trimester of the pregnancy and first year of postnatal life, ischemic WMI could result in exaggerated WM impairment in human children (Baltan et al., 2011). CNS myelination disturbance is a central feature in many conditions ranging from ischemia and cerebral palsy in infants to stroke and multiple sclerosis in adults (Matute, 2011). These resulting conditions can leave affected individuals severely handicapped with little or no recovery prospect, yet no specific pharmacotherapies presently exist (Fern and Matute, 2019).

Brain injury causes elevated glutamate levels in the extracellular space (Jensen, 2005; Beppu et al., 2014) largely due to the reversal of the glutamate transporters (GluT) (Stirling and Stys, 2010). Glutamate is released *via* cystine-glutamate anti-porter activity and vesicular release after depletion of ATP (Matute, 2011; Evonuk et al., 2020). High amounts of glutamate and

Received 16 March 2021, accepted 18 May 2021

© 2021 by Acta Neurobiologiae Experimentalis

the resultant sustained activation of ionotropic glutamate receptors (iGluR) is implicated in subsequent OL and astrocyte death (Salter and Fern, 2005; Volpe, 2009; Canedo-Antelo et al., 2018). In general, it is thought that responsible etiopathogenic mechanisms include glutamate excitotoxicity, elevated Ca^{2+} influx, oxidative stress, release of NO and pro-apoptotic factors that stimulate caspases (Matute, 2011; Sanchez-Gomez et al., 2003; 2011; Back and Rosenberg, 2014).

During development, the WM cellular elements are under attacks (Butt et al., 2014; Fern and Matute, 2019). OL lineage cells are more susceptible to insults than other glial cells (Fern and Matute, 2019). OL lineage cells express Ca^{2+}-permeable iGluRs that make them susceptible to insults (Sanchez-Gomez et al., 2011; Fern and Matute, 2019). Injury to mature and immature OLs leads to myelination loss (Arai and Lo, 2009). After insult, remyelination derives from OPC recruitment and differentiation (Li et al., 2015).

The OLs traverse several steps, from OPC that express a set of markers such as PDGFαR and proteoglycan NG2, to mature OLs that express myelin genes such as myelin-associated glycoprotein (MAG), myelin oligodendrocyte glycoprotein (MOG), myelin basic protein (MBP), 2'-3'-cyclic nucleotide 3' phosphohydrolase (CNP), and proteolipid protein (PLP) (McTigue et al., 2001; Rivers et al., 2008). Regulation of the OL development is multifactorial, and many transcriptional factors including bHLH transcription factors (e.g., Olig1, and Olig2) and a homeobox protein (e.g., Nkx2.2) play roles in the differentiation of OPCs as well as myelin regeneration (Fancy et al., 2004). Therefore, pharmacological drug analysis enhancing myelin repair need to investigate of their impacts on OPC proliferation, expression of myelin genes, and transcriptional factors that regulate the development of OLs as well as re/myelination (Fern and Matute, 2019). In this study, we hypothesized that WM ischemia would activate iGluRs and that treatment with combined (AMPA and NMDA) iGluR block would minimize population OL loss, reduce myelin disruption and inhibit reactive gliosis in an *ex vivo* rat model of WM ischemia.

METHODS

Ethics statement

All animal experiments were carried out in accord with the regulations of the Research Ethics Committee of the Faculty of Biological Sciences at the University of Leeds and under the provisions of the UK Animals (Scientific Procedures) Act 1986.

Cerebellar ex vivo slice culture model

Methods were based on previously published protocols (Stoppini, 1991; Al-Griw et al., 2021). Briefly, brains from 7-day-old Wistar rats (postnatal day 7) were used to generate cerebellar slice tissues that contained developing WM. Pups were sacrificed, and the cerebellum was dissected and transversely sliced at a thickness of 300-µm on a vibratome (Leica, Germany). Eight to ten tissue slices per rat brain (at least 5 animals per each experimental group) were carefully transferred onto humidified 1.0 µm pore size cell culture inserts (Millipore, Falcon, UK) and placed in a 6-well plate (Falcon). The tissues were kept in one ml of serum-based medium (50% minimum essential medium Eagle (MEME, Sigma), 25% HBSS (hanks balanced salt solution, Invitrogen), 20% normal horse serum (Invitrogen), 4.6 mM, (v/v) L-glutamine (Sigma), 21 mM (v/v) D-glucose (Fisher Scientific, UK), 1% penicillin/streptomycin solution (Invitrogen), 4.2 µM (v/v) L-ascorbic acid (Aldrich-Sigma, Germany) and 11 mM (v/v) $NaHCO_3$ at pH 7.2-7.4) in a humidified aerobic incubator (5% CO_2) at 37°C for 3 days.

Induction of white matter injury (WMI)

Ischemic WMI was simulated by exposing 7-day-old cultures to 20 min oxygen-glucose deprivation (OGD) insult. Briefly, the tissue slices were transferred into filter-sterilized, deoxygenated glucose-free culture medium for 20 min in an anaerobic airtight chamber with a mixture of 95% N_2/ 5% CO_2 gas flow, temperature maintained at 37±0.5°C. After OGD-insult, the cultures were washed at least three times with fresh oxygenated culture medium containing 5 mg/ml D-glucose and supplemented with 0.3% B27 and returned to their culture conditions under normoxic atmosphere (5% CO_2) at 37°C. Non-OGD treated cultures (control cultures) were maintained for the same time under normoxic conditions. The cultures were incubated for 3 days before being fixed for analysis.

Experimental group design

The tissue culture slices were randomly allocated to one of 3 groups. Group-I (SHAM) tissue slices were cultured under normoxic conditions at 37±0.5°C at the time-points corresponding to that in other experimental groups. Group-II (WMI) tissue slices were cultured and subjected to 20 min of OGD insult in an atmospheric perfusion airtight chamber (95% N_2/ 5% CO_2) gas flow at 37±0.5°C. After OGD treatment, the cultures were washed three times with normal medium before returning them to normoxic atmosphere for 3 days of reperfusion. Group-III (WMI+-

blockers), cultured tissue slices were subjected to 20 min of OGD insult and then were treated with the blockers or vehicle alone (0.1% DMSO). All test pharmacological agents were added to culture medium 20 min before, during or 20 min after the OGD end and maintained in the culture medium for 60 min. Appropriate control groups were performed at the corresponding time-points with these blockers to test their cytotoxicity.

Drug application

To explore the role of N-methyl-D-aspartate (NMDA) receptor, 10 μM of dizocilpine maleate MK-801, an antagonist of the NMDA receptor, (dissolved in DMSO as 10 mM stock; Tocris, Ellisville, UK) was used. Memantine (dissolved in DMSO as 5 mM stock; Tocris, Ellisville, UK) was also used to block NMDA iGluRs. α-amino-3-hydroxy-5-methylisoxazole-4-propionic acid (AMPA)/kainite GluRs were blocked using 30 μM of 2,3-dihydroxy-6-nitro-7-sulfamoyl-benzo(f)-quinoxaline 2,3-dione (NBQX, 30 μM; Tocris, Ellisville, MO; dissolved in dissolved in DMSO as 30 mM stock). Nifedipine (Acros Organics, UK), a blocker of L-type Ca^{2+} channels was dissolved in DMSO as 10 mM stock. The involvement of reversal GluTs in OGD-induced damage, as important glutamate release source was tested using 200 μM of DL-TBOA (Tocris Elliville, MO; dissolved as 100 mM stock in 100 mM NaOH stock). All drugs were stored at -20°C prior to use.

Glutamate assay

The released glutamate from cultured cerebellar slices into superfusate was measured using an enzymatic assay (glutamic acid/glutamate oxidase assay, Invitrogen, UK). In brief, 50 μl of diluted L-glutamate-containing samples from each well was transferred to separate wells of a fluorescence microplate reader and mixed with 50 μl of 100 μM Amplex®Red reagent containing 0.25 U/ml horseradish peroxidase (HRP), 0.08 U/ml L-glutamate oxidase, 0.5 U/ml L-glutamate-pyruvate transaminase, and 200 μM L-alanine at 37°C for 45 min. Optical densities were measured using excitation at 530-560 nm and emission detection at 590 nm. Glutamate concentrations in experimental samples were calculated by comparison with a standard glutamate solution.

Cell survival assay

Cell survival was measured using a Live/dead Viability/Cytotoxicity kit in accordance with manufacturer's instructions (Molecular Probes, Invitrogen, UK). Briefly, tissue slices were further incubated in the presence of a combined solution containing 4 μM ethidium homodimer-AM (EthD-1) and 2 μM calcein-AM (Cal) at 37°C for 30-45 min, and were then fixed in 4% paraformaldehyde (PFA, Sigma, UK) in phosphate-buffered saline (PBS, Oxoid, UK) for 30 min at room temperature. Using confocal microscopy, viable cells showed the green fluorescence of Cal and dead cells showed the red fluorescence of EthD-1.

TUNEL assay

Apoptosis was identified at single cell level based on labeling of DNA strand breaks using TUNEL (terminal deoxynucleotidyl transferase-mediated dUTP digoxigenin nick-end labeling OH ends in genomic DNA with Fluorescein) detection kit in accordance with manufacturer's recommendation (Chemicon, ApopTag Fluorescein in Situ Apoptosis Detection kit, UK). Briefly, tissue slices prepared and cultured as described above, were then fixed with 4% PFA in PBS for 30 min at room temperature. The fixed slices were incubated in working strength terminal deoxynucleotidyl transferase (TDT) enzyme for 1 h at 37°C in the dark, and the reaction was stopped by stop/wash buffer. DAPI (4, 6-diamidino-2-phenylindole, Vector Laboratories, UK) was applied to stain nuclei. Non-specific staining was examined by omission of the TDT in the labeling procedure.

Cell proliferation studies

Cell proliferation was determined by using the DNA replication marker BrdU (5-bromo-2`-deoxyuridine, Aldrich-Sigma, UK). Cultured tissue slices were incubated in medium containing 20 μM BrdU for 3 or 24 h prior to fixation. The fixed cultures were incubated with 1N HCL for 10 min on ice followed by 10 min incubation with 2N HCL at room temperature before placing them in an incubator at 37°C for 20 min. To neutralize acid, slices were incubated with borate buffer (0.1 M, pH=8.5) for 12 min at room temperature, followed by three 5 min washes in PBS with 1% Triton 100-X. The slices were subsequently permeabilized in a solution containing PBS (1M) with 1% Triton 100-X, glycine (1 M) and 5% normal goat serum for 1 h prior to incubation overnight with anti-BrdU mono-antibody (eBioscience, UK) at a dilution 1:50 in PBS followed by DAPI labelling of nuclei. The proliferating ($BrdU^+$/$DAPI^+$) cells were then counted.

Immunocytochemistry

For immunocytochemical analysis, the cultured slices were fixed in 4% PFA in PBS for 60 min at room

temperature. Following 3 washes with PBS; the slices were mounted on glass and were then blocked for 1 h at room temperature with a serum blocking solution (10% normal goat serum (MP Biomedical), 0.25% Triton 100-X (Sigma, UK) in PBS. Primary antibodies were diluted in PBS and were then incubated for 24 h at 4°C in the dark. The slices were washed 3 times for 5 min in PBS and secondary antibodies diluted in PBS were added for 2 h at room temperature in the dark followed by three washes in PBS. The sections were incubated with 100 µl of primary antibody (anti-MBP; anti-NG2, Millipore, and Anti-NF200; Sigma) for 90 min at room temperature or overnight in dark at 4°C. The sections were then washed three times for 5 min in PBS, stained with secondary antibodies (Alexa Fluor® 633 and 488) (Invitrogen, Germany), which were diluted in PBS (1:1000), for two hours at room temperature in the dark, and then washed three times in PBS. DAPI was used for morphological assessment of nuclei. To determine the specificity of immunolabelling with the antibodies, control tissues were processed without primary antibodies, which resulted in no immunostaining.

Assessment of WM element injury

Imaging of immunostained slices was performed by inverted Zeiss LSM 510 Meta confocal laser scanning microscope with HeNe and argon lasers (Carl Zeiss, Inc., Germany) with confocal configuration 405 nm (DAPI, blue), 488 nm (FITC, green), 543nm (rhodamine, red), and 633 nm (cy5, red) fluorescence.

To quantify myelination (myelin-axon alignment), immunofluorescence double labeling of MBP (myelin basic protein) protein, and its alignment with NF (neurofilament) protein was performed. A series of immunofluorescence images were gathered in the z-axis from a confocal microscopic field in the midline of each tissue section using a 63X oil immersion objective lens. The confocal images were randomized and divided into a 5×5 grid. The images were scored by a blind observer. Percent of myelination of axons was measured across a minimum of 9 predetermined grid sections outlined by hand using imageJ. The length of each axon was measured based on NF-staining, as was the length of the axon that showed colocalisation with MBP. The proportion of the axon showing colocalisation with MBP was then calculated. The number from 3 images were averaged and used as damage score of a single section.

Injury to OLs was evaluated by counting total number of MBP^+ OLs as well as the percent of apoptosis among OL population by a blinded observer to the experimental conditions as described previously (Mangin et al., 2012). Morphological characteristics of pyknotic OLs were also counted. Apoptosis among OL population were determined and counted based on morphological characteristics as previously described (Back et al., 2002).

Cell quantification pixel intensity measurement

Immunopositive cells were counted in 5 randomly selected fields per slice with 3 slices per animal per condition with at least 4 independent biological replicates under 63X magnifications using 9 predetermined grid sections outlined manually using ImageJ (National Institutes of Health, MA, http://rsb.info.nih.gov/ij/) with a grid size, 400 × 300 µm; counting frame, 25 × 25 µm; z-depth 50 µm.

Quantitative analysis of the immunoreaction intensity (pixel intensity) was performed in a series of confocal immunofluorescence images (z-depth 50 µm) at 40× magnification (1024 × 1024 pixels) using ImageJ as previously described (Olivier et al., 2009).

Expression studies

RNAs were isolated from the cultured tissues using TRIzol (Invitrogen, UK), and cDNA was synthesized with Super Script II reverse transcriptase (Invitrogen). Quantitative real-time reverse transcriptase polymerase chain reaction (Q-RT-PCR) was carried out with a Rotor Gene 6000 PCR analyzer (Corbett Research, UK) with primers described in Table 1. Specificity of PCR amplification and the absence of primer dimers were confirmed by analysis of cycling and melting curves. To further confirm appropriate amplification, the size of amplicons (PCR products) was verified on gel electrophoresis and sequencing. Transcript levels were normalized to the housekeeping U6.

Statistical analysis

Findings were analyzed using the SPSS version 20.0 Statistical Package for Social Science (SPSS Inc., Chicago, IL, USA). All data represent the mean±SEM for at least 5 independent experiments performed in triplicate. Normality was assessed using the computerized Kolmogorov-Smirnov test. One way analysis of variance (ANOVA) followed by a post-hoc test for multiple comparisons Dunnett's were used to determine statistical significance between the studied groups. P values<0.05 were considered statistically significant.

Table 1. Rat mRNA primer sequences used for Q-RT-PCR.

Gene	Reverse primers (5`-3`)	Forward primers (5`-3`)	Amplicon Size	Source
U6	aacgcttcacgaatttgcgt	ctcgcttcggcagcaca	120 bp	Eurogenetic
NG2	gctcacagaatattcccagca	cagaggaggctttggtgaac	63 bp	Sigma
MAG	caggcgcttctcactctca	tcctgtacagccccgaat	65 bp	Sigma
MOG	cacggcggcttcttcttggt	gtctatcggcgagggaaaggt	121 bp	Sigma
MBP	tgtgcttggagtctgtcacc	ccgcctcagaagacagtgat	96 bp	Sigma
PLP	ctgccagtctattgccttcc	agcattccatgggagaacac	94 bp	Sigma
CNP	aaattctgtgactacgggaagg	ccgtaagatctcctcaccaca	74 bp	Sigma
Gap-43	cgggcactttccttaggttt	cggagactgcagaaagcag	76 bp	Sigma
Olig1	tgggtttcggagtggaga	gcgagcctgaaagacagaac	60 bp	Sigma
Olig2	cccctcccaaataactcaaac	gaaatggaataatcccgaactact	86 bp	Sigma
Nkx2.2	tgtgctgtcgggtactggg	cgggctgagaaaggtatgga	96 bp	Sigma
BDGαR	agaaaaaggttaaaacccacctaag	cacacgccacgtacatcc	96 bp	Sigma
SOX10	agactgactgagcgactgagc	tgtcctcctcacccttcttg	91 bp	Sigma
Cas-1	cacaagaccaggcatattctttc	tgctttctgctcttcaacacc	110 bp	Sigma
Cas-3	catgacccgtcccttgaa	ccgacttcctgtatgcttactcta	70 bp	Sigma
Cas-8	tcacatcatagttcacgccagt	agagcctgagggaaagatgtc	72 bp	Sigma
Cas-9	gagcatccatctgtgccata	cgtggtggtcatcctctctc	81 bp	Sigma
BDNF	ccttttctggtttgcaatgag	cgaggttggaacctaacagc	68 bp	Sigma

RESULTS

Ex vivo cerebellar slices model replicates ischemia-induced WMI

To test the adequacy of *ex vivo* cerebellar slices model for investigation of ischemia-induced WMI, glutamate release levels in cerebellar slice culture medium was measured. Baseline level of glutamate was measured for 20 min prior to OGD or inhibitor by sampling small volumes of cell supernatant from each well at serial time points. For comparison, data were normalized to the average glutamate levels of control slice cultures, which ranged from 60-70 nM and remained constant under normoxia. The results show that glutamate release began a few minutes after the OGD-insult (Fig. 1A), and peaked (10-fold higher compared with basal levels) 20 min after WMI end (Fig. 1A). The data also showed that long-term effects of OGD-induced glutamate release can continue days after the insult (Fig. 1A). The increase in the levels of glutamate was significantly reduced in culture medium of OGD-treated slices treated with DL-TBOA, an inhibitor of glutamate transporter (Fig. 1A-C).

Inhibition of iGluR signaling enhances cell survival upon WMI

Because of inhibition of AMPA and NMDA receptors alleviates Ca^{2+}-mediated excitotoxicity and cell death (Fern and Matute, 2019), we reasoned that inhibition of AMPA and/or NMDA receptors might enhance cell survival of WM elements after injury. To this end, we measured cell survival after OGD in cultures exposed to the iGluR blockers. We found that cell survival was lower in the WMI group compared to SHAM group and that iGluR block preserved cell survival (Fig. 2B). Specifically, the protection induced by NBQX in combination with either MK-801 or memantine was greater that observed with any single inhibitor used alone (Fig. 2B).

Considering the practical need for an effective treatment following an ischemic attack and in order to elucidate the mechanism of this anti-excitotoxic treatment, we tested the impacts of MK-801+NBQX when added for a 60 min period beginning 20 min after WMI. A 20 min post-injury treatment with MK-801+NBQX was not as effective as immediate treatment but resulted in a significant reduction in WM damage (Fig. 2C).

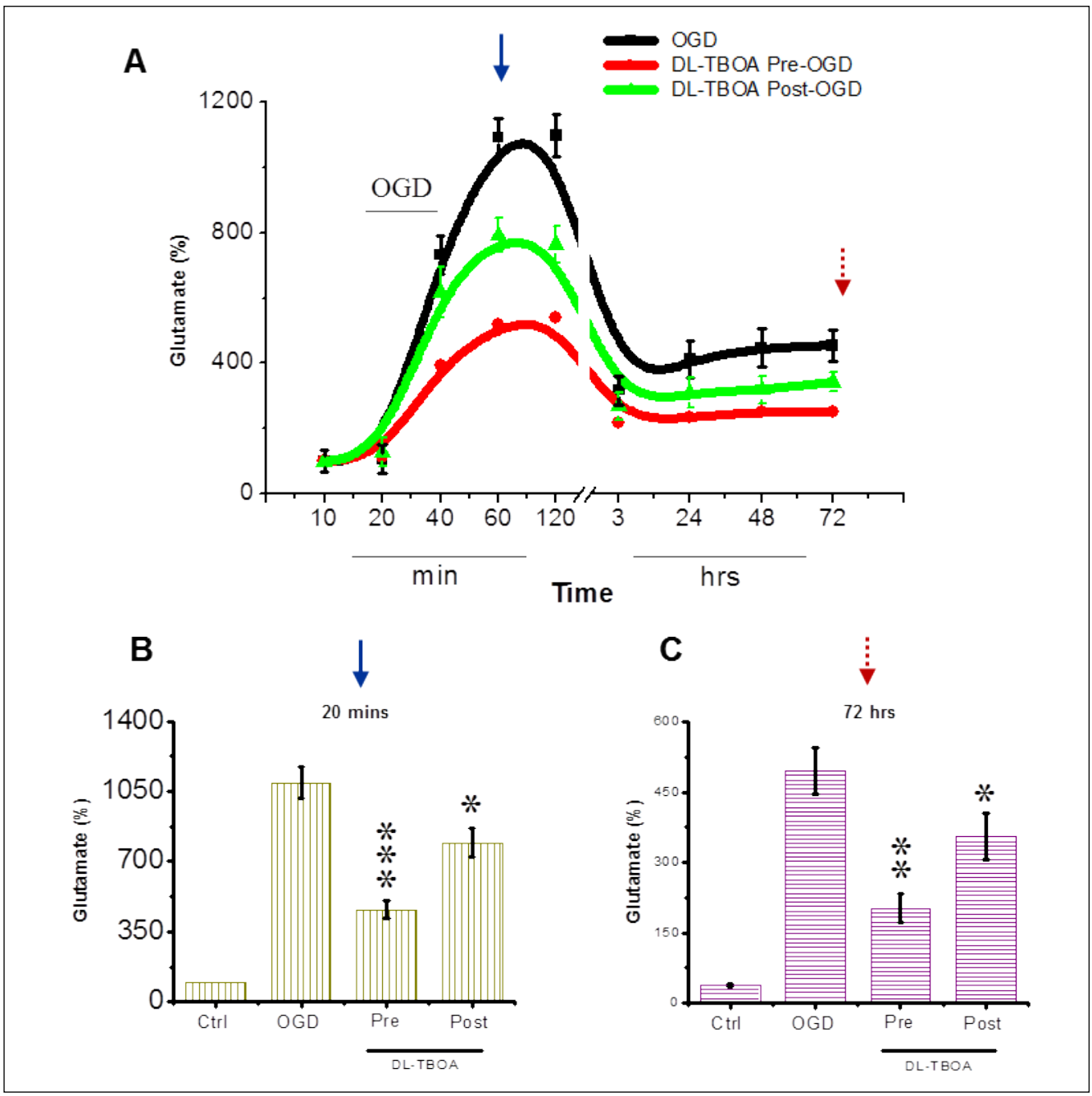

Fig. 1. Time course analysis of glutamate release after WMI. (A) represents the corresponding levels of glutamate released in the culture medium of cerebellar slices. Glutamate levels were measured, and expressed as the percentage of control. (B) and (C) show levels of glutamate quantified at 20 min and 72 h in post-OGD DL-TBOA treatment. Data are presented as mean ± SEM of 8 to 10 tissue slices/animal at least 5 animals/ each experimental group. (*) indicates $P<0.05$, (**) indicates $P<0.01$, and (***) indicates $P<0.001$.

Inhibition of iGluR signaling reduced apoptosis upon WMI

We next asked whether treatment with MK-801+NBQX-induced protection after WMI involved changes in apoptosis. To this end, TUNEL assay in combination with DAPI-nuclei labelling was carried out. We found that apoptotic (TUNEL$^+$) cells were more abundant in the WMI group compared to SHAM group (Fig. 3A), and that pre-treatment with MK-801+NBQX substantially reduced their density (Fig. 3B). Interestingly, post-treatment with MK-801+NBQX was also effective in enhancing cell survival after WMI (Fig. 3B). Taken together with the data presented in Fig. 2, these find-

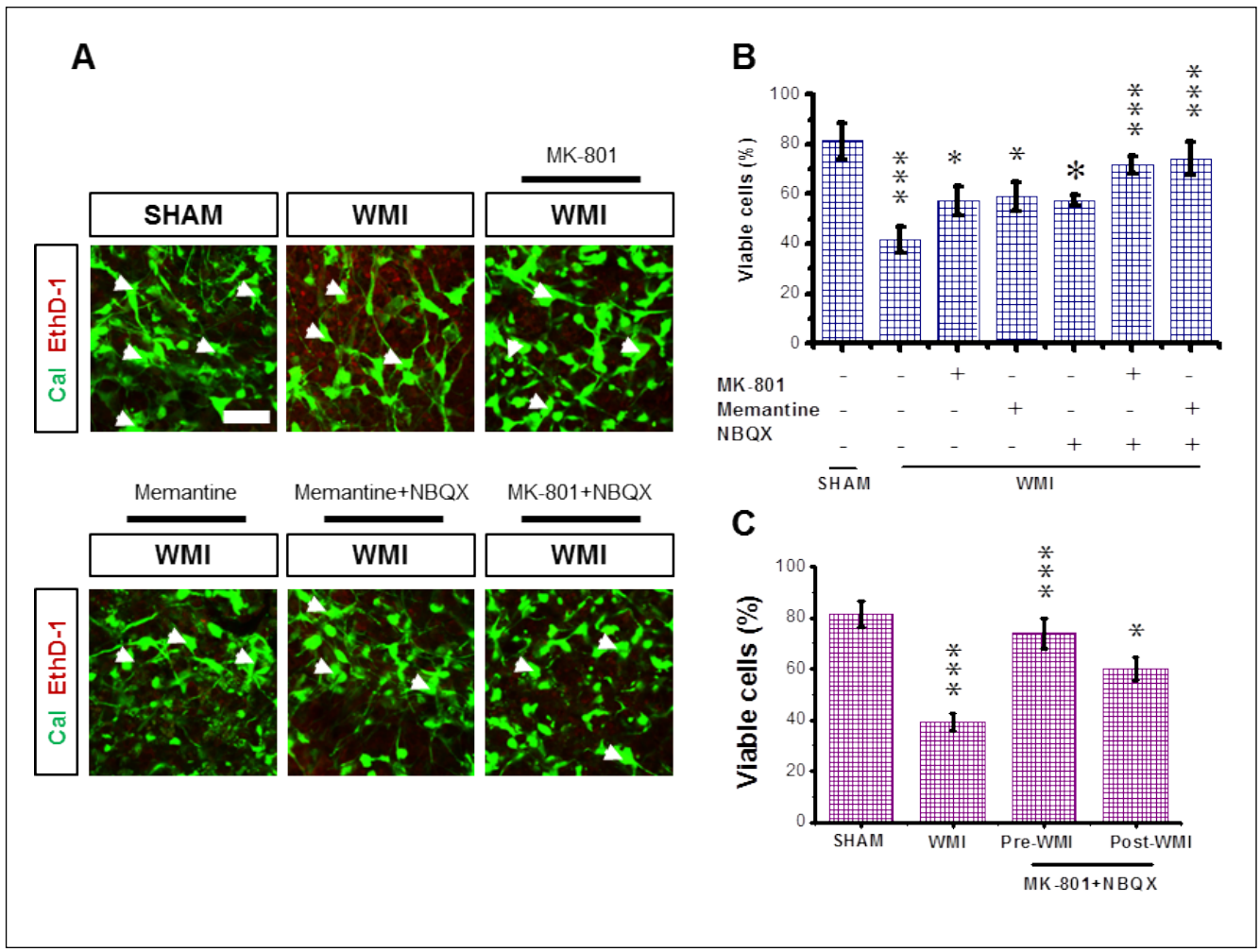

Fig. 2. MK-801+NBQX treatment enhances cell survival after WMI. Cultured cerebellar slices were exposed to conditions of SHAM, WMI, or WMI+MK-801+NBQX. (A) Representative immunofluorescence images of viable cells (green fluorescence of calcein-AM, Cal) and dead cells (red fluorescence of ethidium homodimer-AM, EthD-1). Scale bar: 30 μm. (B) Quantification of viable cells. (C) Quantification of viable cells pre- and post-treatment with MK-801+NBQX after WMI. Data are presented as mean ± SEM of 8 to 10 tissue slices/animal at least 5 animals/ each experimental group. (*) indicates $P<0.05$ and (***) indicates $P<0.001$.

ings indicate a consistent protection conferred by post-injury treatment with MK-801+NBQX and suggests a window of opportunity to attenuate WMI therapeutically.

Prolonged activation of iGluR signaling can activate caspases (Matute et al., 2006) and their activation is considered a commitment to apoptotic cell death (Nicholson et al., 1995; Cohen, 1997). To investigate the molecular pathway/s involved in WMI-mediated apoptosis, we measured the expression of caspase-9, caspase-8, and caspase -3 by Q-RT-PCR. Gene expression studies demonstrated that caspase-9, caspase-8, caspase -3 mRNA expression levels were upregulated (Fig. 3C-E). This suggests that WMI-induced, caspase-mediated apoptosis, in this model, was *via* the iGluR signaling pathway.

Inhibition of iGluR signaling restores OLs and myelination upon WMI

Because iGluR activation mediates OL death, inhibits OPC maturation, and myelination in hypoxia-ischemia models (Volpe, 2009; Doyle et al., 2018; Fern and Matute, 2019), we reasoned that inhibition of iGluR signaling might protect OL development and myelination. To this end, we immunostained the cultured slice sections with antibody to MBP. At 3 days post-WMI, there was a 50% reduction in the average number of MBP^+ OLs compared to SHAM group (Fig. 4A-B), and that combined iGluR block (MK-801+NBQX) enhanced the counts of MBP^+ OLs ($P=0.002$, 103.91±8.96 cells per field; Fig. 4A-B). Moreover, Q-RT-PCR results demonstrated that MAG, MOG, CNP, PLP, MBP, and GAP-43 mRNA ex-

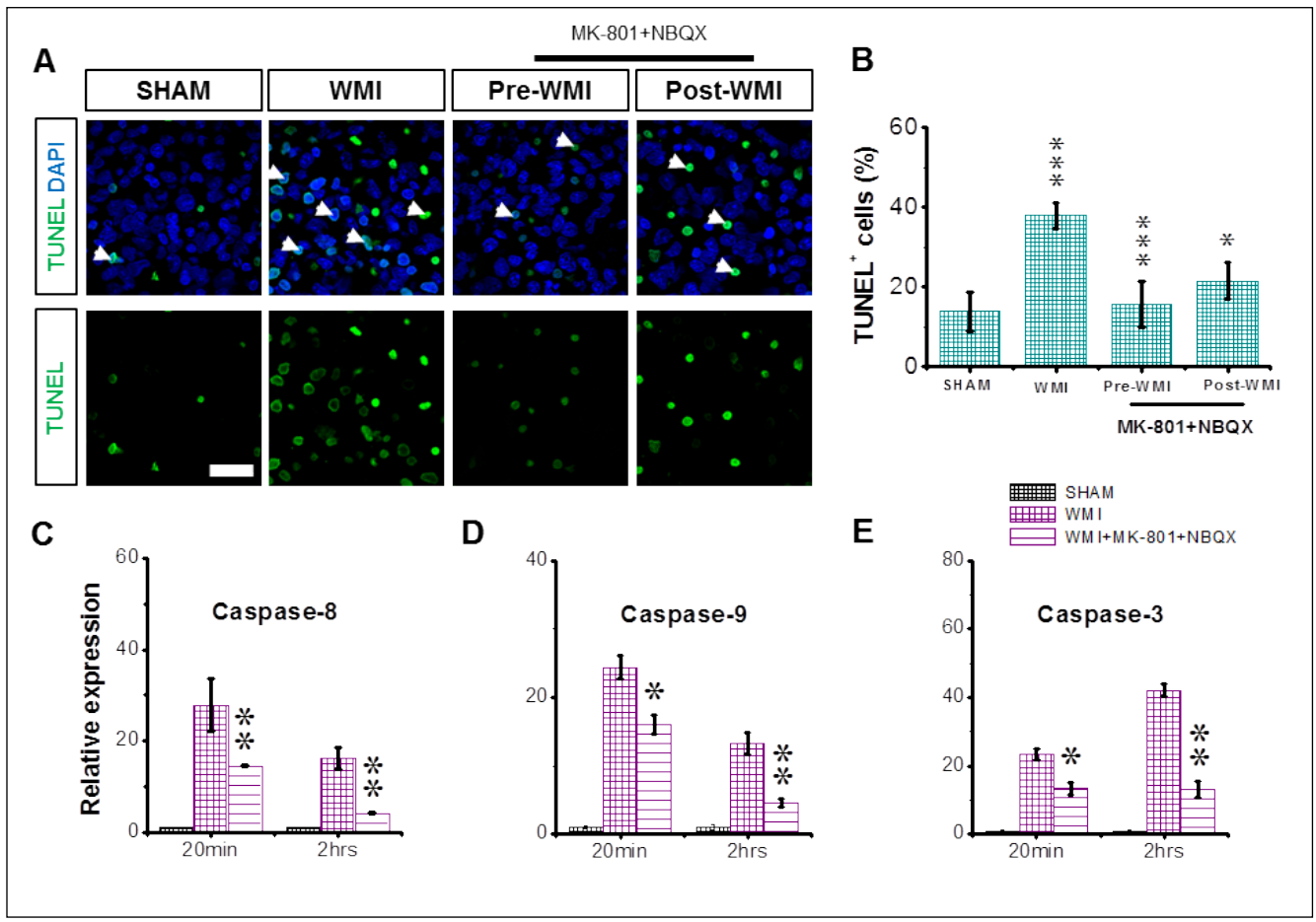

Fig. 3. MK-801+NBQX treatment minimizes delayed cell death after WMI. Cerebellar slices were cultured and exposed to conditions of SHAM, WMI, or WMI+MK-801+NBQX. (A) Representative immunofluorescence images for TUNEL (green) and for DAPI-labelled nuclei (blue). Sale bar: 20 μm. (B) Quantification of TUNEL⁺ cells. Relative mRNA expression levels for (C) caspase-8, (D) caspase-9, (E) caspase-3. Data were normalized for the mean of the relative expression of to U6. Expression levels are presented relative to levels in SHAM group, where were set at 1. Data are presented as mean ± SEM of 8 to 10 tissue slices/animal., at least 5 animals/ each experimental group. (*) indicates $P<0.05$, (**) indicates $P<0.01$, and (***) indicates $P<0.001$.

pression levels were reduced in WMI group compared to SHAM group (Fig. 4C-G), suggesting an ongoing myelin disruption, and that MK-801+NBQX treatment significantly upregulated MAG, MOG, CNP, PLP, and MBP expression, but not an axonal regeneration marker GAP-43 in WMI group (Fig. 4C-G). This is consistent with a high cell survival.

Next we asked whether MK-801+NBQX treatment declined apoptosis among MBP⁺ OLs in this model. To this end, we double-labeled the cultured slice sections for TUNEL and MBP antigen (Fig. 4H). We found that apoptotic MBP⁺ OLs were more abundant in the WMI group compared with SHAM group (Fig. 4I), and that MK-801+NBQX treatment substantially reduced the density of apoptotic MBP⁺ OLs (Fig. 4I).

We next evaluated the impacts of blocking iGluR signaling on myelination after WMI. To this end, we determined at which day of *ex vivo* myelination (myelin-axon alignment) was high enough to reliably study the impacts of WMI on the status of myelination as a measure of WM damage. During rodent brain development, myelination is not easily detectable in the first postnatal week. However, at the second and third postnatal weeks, there is an increase expression in MBP and NF. We measured MBP and NF expression over time in our *ex vivo* model. We found that myelin-axon alignment gradually increased from 6 to 7 days in culture, which is an equivalent in maturation stage to the human fetus. The impacts of WMI on the integrity of myelin-axon colocalisation were therefore measured at 7 days in culture followed by 3-days reperfusion (Fig. 5A). No MBP-NF loss was seen in SHAM group (Fig. 5A-B). The OL morphology conformed to prior descriptions, characterized by primary process running parallel to axons (Butt and Ransom, 1993; Salter and Fern, 2005). At 3 days post-WMI, there was a marked decrease in the

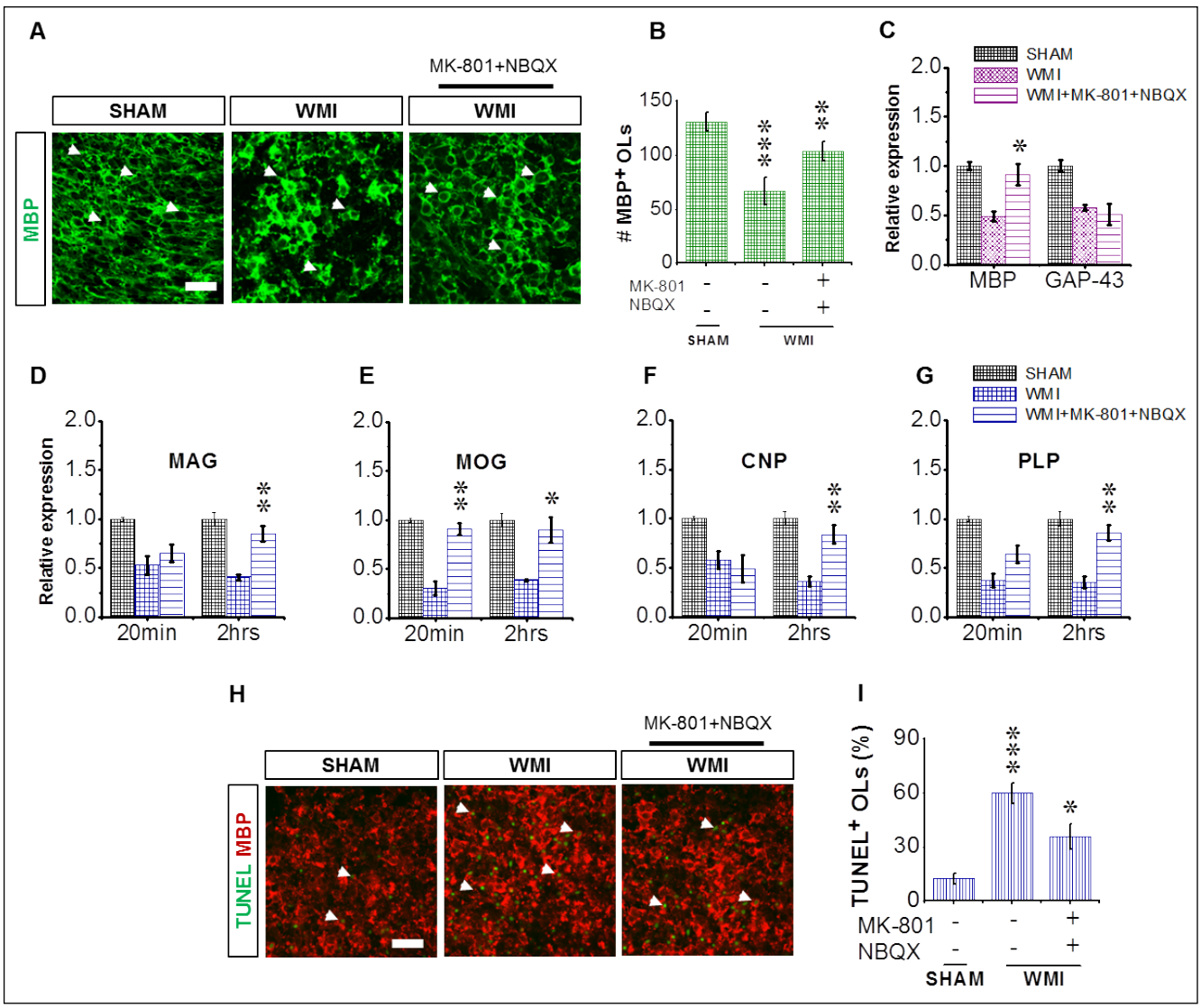

Fig. 4. MK-801+NBQX treatment mitigates OLs after WMI. Cerebellar slices were cultured and exposed to conditions of SHAM, WMI, or WMI+MK-801+NBQX. (A) Representative immunofluorescence images of MBP+ OLs (arrowheads, green). Scale bar: 20 μm. (B) Quantification of MBP⁺ OLs. Relative mRNA expression levels for (C) MBP and GAP-43 and for myelin genes (D) MAG, (E) MOG, (F) CNP, and (G) PLP at 2 and 2 h after WMI. Data were normalized for the mean of the relative expression of U6. Expression levels are presented relative to levels seen in SHAM group, where were set at 1 (H) Representative images of TUNEL (green) and MBP immunostaining for OL (red). Scale bar: 20 μm. (I) Quantification of TUNEL⁺/MBP⁺ OLs. Data are presented as mean ± SEM of 8 to 10 tissue slices/animal at least 5 animals/ each experimental group. (*) indicates $P<0.05$, (**) indicates $P<0.01$, and (***) indicates $P<0.001$.

myelin-axon colocalisation (demyelination) compared to SHAM (Fig. 5A-B), and that MK-801+NBQX protected myelinated axons after WMI (Fig. 5A-B). Together, these findings demonstrate that efficacy of iGluR blockers in preserving WM integrity after an ischemic injury.

OL development and remyelination are modulated by key factors such as PDGFRα, Olig1, Olig2, Nkx2.2, Sox10 and NG2 (Fancy et al., 2011). Olig2 and Nkx2.2 are required for the expression of the major protein components of myelin; MBP, MAG, and PLP (Fu et al., 2002). Here we postulated that MK-801+NBQX treatment might affect the expression of these factors. To this end, we measured PDGFαR, NG2, Olig2, Sox10, Nkx2.2, and Olig1 mRNA expression. We found that PDGFRα, NG2, Olig2, Sox10, Nkx2.2, and Olig1 expression were downregulated in WMI group compared to SHAM group, as measured by Q-RT-PCR, (Fig. 5C-G). This lower expression correlates with fewer numbers of OLs. On the other hand, MK-801+NBQX treatment significantly upregulated PDGFRα, NG2, Olig2, Sox10, Nkx2.2, and Olig1 expression in WMI group (Fig. 5C-G). Taken together with the data presented in Fig. 4B, these results indicate that maintained the OL population which is reflected in more mRNA expressed OL cells.

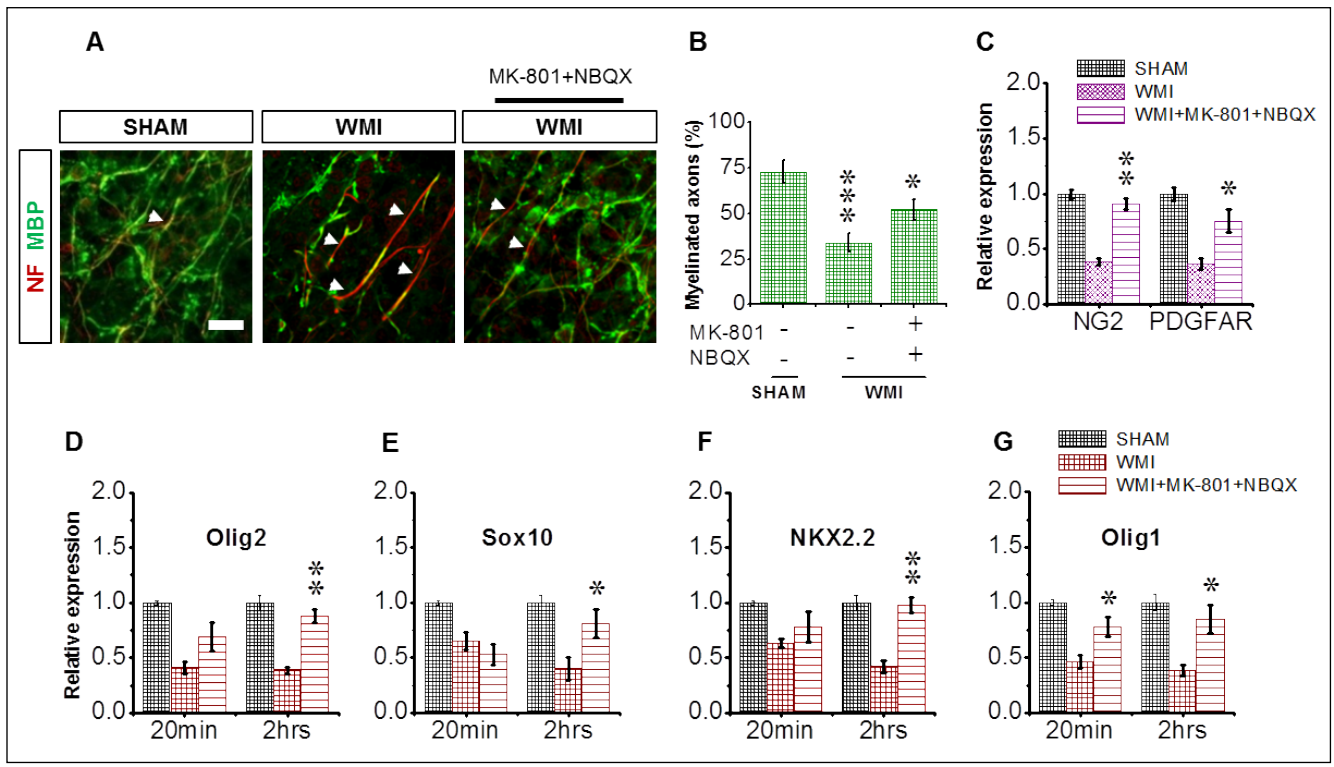

Fig. 5. MK-801+NBQX treatment restores myelination after WMI. Cerebellar slices were cultured and exposed to conditions of SHAM, WMI, or WMI+MK-801+NBQX. (A) Representative immunofluorescence images for MBP (green) and for NF (red). Arrowheads indicate demyelinated axons. Scale bar: 50 μm. (B) Quantification of myelinated axons from (%) Relative mRNA expression levels for (C) PDGFαR and NG2, (D) Olig2, (E) Sox10, (F) Nkx2.2, and (G) Olig1. Data were normalized for the mean of the relative expression of to U6. Expression levels are presented relative to levels seen in SHAM group, where were set at 1. Data are presented as mean ± SEM of 8 to 10 tissue slices/animal at least 5 animals/ each experimental group. (*) indicates $P<0.05$, (**) indicates $P<0.01$, and (***) indicates $P<0.001$.

Inhibition of iGluRs enhances OPC survival and maturation upon WMI

Here we investigated the impacts of iGluR inhibition on OPC survival in our *ex vivo* slice model of developing WMI. To this end, we immunostained the cultured cerebellar slice sections with antibody to NG2, an early OPC marker. Under SHAM condition, there were a high number of $NG2^+$ OPCs (Fig. 6A). The morphology of OPCs conformed to prior descriptions, characterized by small, irregular, rounded, cell bodies with a few short processes, highly branched (Levine and Card, 1987). At 3 days post-WMI, there was a roughly 60% reduction in the average number of $NG2^+$ OPCs compared to SHAM group (Fig. 6A-B), and that MK-801+NBQX treatment enhanced the counts of $NG2^+$ OPCs (Fig. 6A-B).

To determine the role for apoptosis in regulating $NG2^+$ cell number, we double-immunostained the cultured tissue sections for TUNEL and NG2 antigen (Fig. 6C). We found that apoptotic $NG2^+$ OPCs were more abundant in the WMI group compared to SHAM group, and that MK-801+NBQX treatment substantially reduced the density of apoptotic $NG2^+$ cells (Fig. 6D) suggesting that WMI promoted apoptosis among $NG2^+$ OPCs.

Because MK-801+NBQX treatment enhanced myelination in our *ex vivo* model WMI, we postulated that MK-801+NBQX treatment might also affect OPC proliferation. To evaluate OPC proliferation, we double-immunostained the cultured cerebellar slice sections for BrdU and NG2 antigen (Fig. 6E-F). We found that proliferating $NG2^+$ OPCs were less abundant in the WMI group compared to SHAM group, and that MK-801+NBQX treatment substantially increased their density (Fig. 6F).

In many models of injury-induced myelination disturbances, myelin regeneration occurs due to OPC proliferation and differentiation (Suyama et al., 2007). To assess the impacts of the MK-801+NBQX treatment on $NG2^+$ OPC maturation, we used BrdU pulse-chase experiment (Fig. 7A). After subjection to WMI condition, the cultured slices were exposed to a 3-h BrdU pulse, and were then either fixed or maintained for a further 3 days (Fig. 7A). Combined iGluR block (MK-801+NBQX) was applied 20 min after the end of OGD insult, and maintained for 60 min. The fixed cultures were

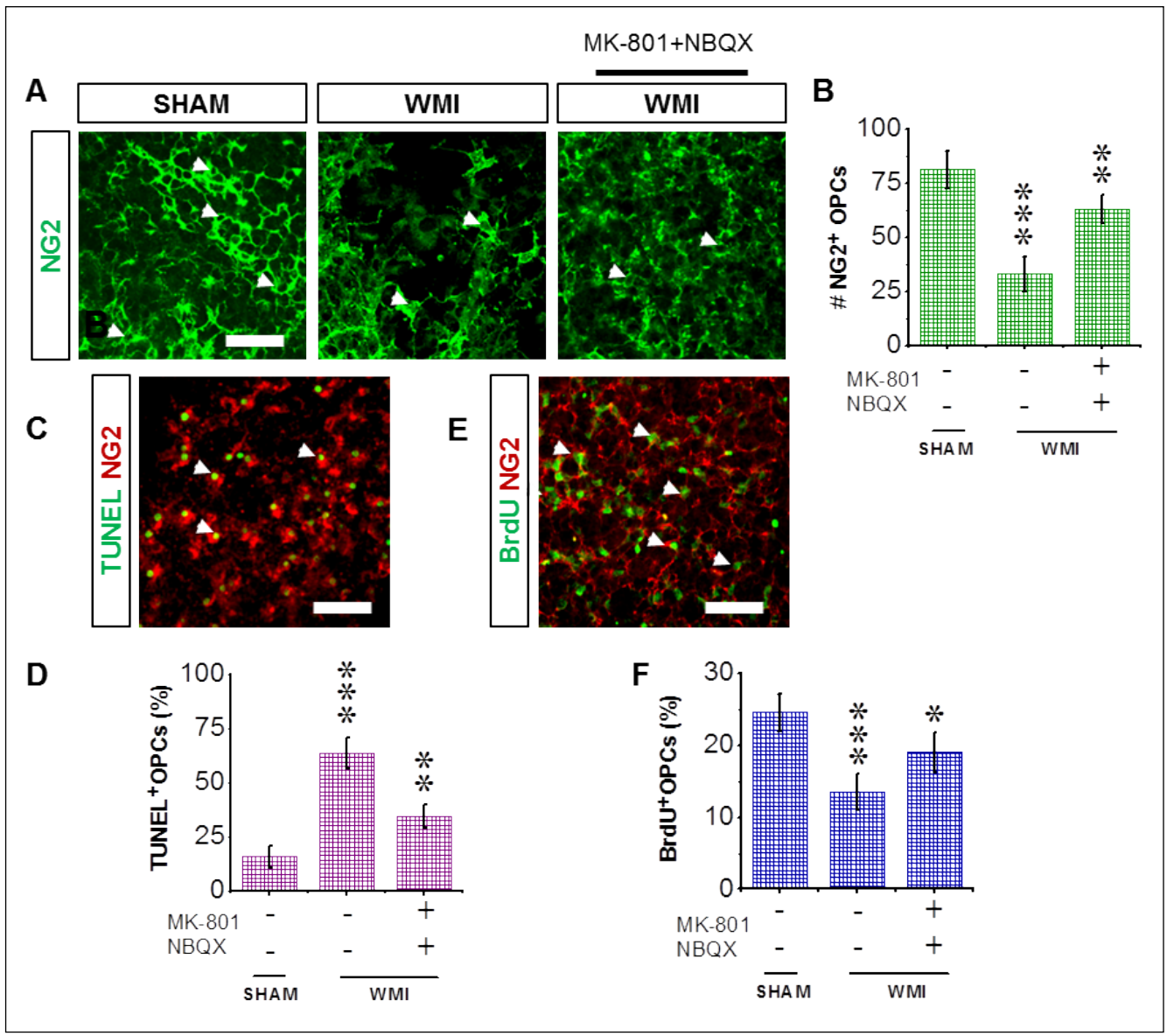

Fig. 6. MK-801+NBQX treatment reduces apoptosis and promotes OPC proliferation after WMI. Cerebellar slices were cultured and exposed to conditions of SHAM, WMI, or WMI+MK-801+NBQX. (A) Representative immunofluorescence images of NG2⁺ OPCs. Scale bar: 20 μm. (B) Quantification of NG2⁺ OPCs. (C) Representative immunofluorescence images for TUNEL (green) and for NG2 immunostaining for OPCs (red) Scale bar: 20 μm. (D) Quantification of TUNEL⁺/NG2⁺ OPCs. (E) Representative immunofluorescence images for BrdU (green) and for NG2 (red). Scale bar: 20 μm. (F) Quantification of BrdU+/NG2⁺ OPCs. Data are presented as mean ± SEM of 8 to 10 tissue slices/animal at least 5 animals/ each experimental group. (*) indicates $P<0.05$, (**) indicates $P<0.01$, and (***) indicates $P<0.001$.

co-stained for BrdU with NG2 antigen (Fig. 7B) or BrdU with MBP (Fig. 7C). After the 3 h pulse-chase, incubation with MK-801+NBQX showed higher NG2⁺ OPCs with BrdU⁺ nuclei (Fig. 7D). However, there were no post-mitotic MBP⁺ OLs with BrdU⁺ nuclei following the 3-h pulse (Fig. 7D). After the 3-day chase period, the fraction of BrdU⁺ OPCs reduced and BrdU⁺/MBP⁺ emerged indicating that these differentiated cells were derived from cells proliferating during the 3 h post-OGD. MK-801+NBQX treatment enhanced the density of BrdU⁺/MBP⁺ OLs in the demyelinated cerebellar slices subjected to WMI condition (Fig. 7E). This suggests that MK-801+NBQX treatment restores OPC maturation in our *ex vivo* model of WMI.

Inhibition of iGluRs suppresses proinflammatory action upon WMI

Her we asked whether combined iGluR block-induced OL and myelin protection after WMI involved changes in the status of inflammation in our *ex vivo* rat

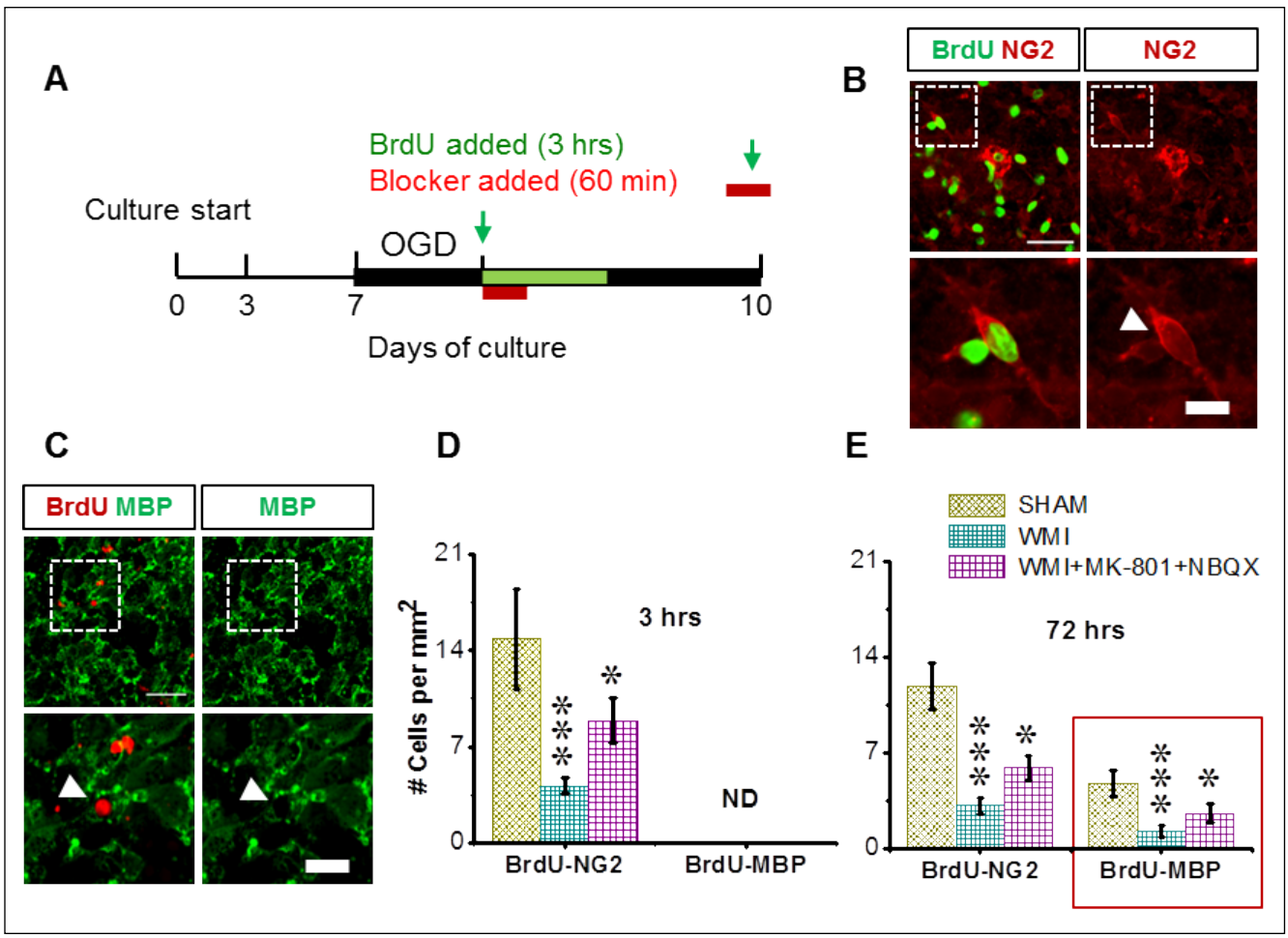

Fig. 7. MK-801+NBQX treatment enhances OPC maturation after WMI. Cerebellar slices were cultured and exposed to conditions of SHAM, WMI, or WMI+MK-801+NBQX. (A) Schematic of OPC maturation assay. (B) Representative immunofluorescence images of DNA replication marker BrdU (green) and OPC marker NG2 (red). (C) Representatives immunofluorescence images for BrdU (red) and for MBP (green) demonstrated that new mature myelinating MBP$^+$ OLs (arrow) are present 3 days after injury in the slices treated with MK-801+NBQX, but not all BrdU$^+$ cells undergo OL differentiation. Scale bar: 40 µm. (D) Quantification of BrdU$^+$ NG2$^+$ OPCs at 3 and 72 h after WMI. (E) Quantification of BrdU$^+$/MBP$^+$ OLs at 3 and 72 h after WMI. ND: not detected. Data are presented as mean ± SEM for at least 5 independent biological replicates. (*) indicates $P<0.05$ and (***) indicates $P<0.001$.

model of developing WMI. We found that a marked increase in the TNF-α, IL-6, IL-1α, IL-1β, and iNOS mRNA expression levels as revealed by Q-RT-PCR (Fig. 8). This finding correlates negatively with OL and OPC survival as show earlier (Fig. 5 and Fig. 6). More importantly, combined iGluR block was also effective in downregulating the TNF-α, IL-1β, and iNOS mRNA expression levels, but not IL-6 and IL-1α (Fig. 8). Because combined iGluR block suppresses proinflammatory action in WMI group, we reasoned that this might influence survival of OL lineage cells and myelination.

DISCUSSION

The novel findings in this work were that post-treatment with combined iGluR block (MK-801+NBQX) alleviated WM pathology and inflammation. Specifically, combined iGluR block decreased OPC apoptosis, promoted OPC maturation, and enhanced remyelination in this model system of WMI. Our findings also demonstrate that combined iGluR inhibition after WMI protects OL lineage cells and myelination, and downregulation the mRNA expression of cytokines and iNOS. Hence, the current work highlights the role of iGluR signaling in WMI and suggests a neuroprotection strategy for neonatal WMI.

WMI takes place at several distinct sites including axons and OLs, microglia, and astrocytes. During ischaemic injury, a plausible mechanism of excitoxicity is the reversal Na^+-dependent GluTs (Baltan et al., 2011; Butt et al., 2014; Fern and Matute, 2019). Astrocytes express high levels of the Na^+-dependent GluT, and injury leads to dissipation of the transmembrane Na^+ gradient

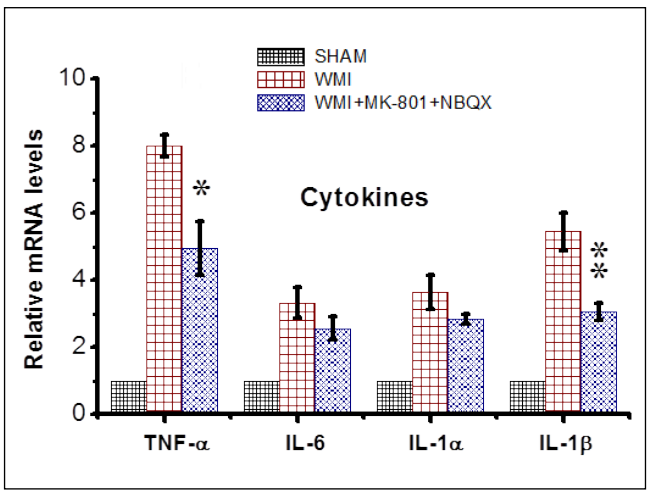

Fig. 8. MK-801+NBQX treatment suppresses proinflammatory action after WMI. Cultured cerebellar slices were exposed to conditions of SHAM, WMI, or WMI+MK-801+NBQX. Relative mRNA expression for TNF-α, IL-6, IL-1α, IL-1β, and iNOS at 20 min post-insult. Data were normalized for the mean of the relative expression of to U6. Expression levels are presented relative to levels seen in SHAM group, where were set at 1. Data are presented as mean ± SEM for at least 5 independent biological replicates. (*) indicates $P<0.05$ and (***) indicates $P<0.001$.

in astrocytes (Fern and Matute, 2019) setting up conditions for reverse exchange as well as glutamate release (Baltan et al., 2011; Butt et al., 2014). In the present study, we found that WMI induced a high amount of glutamate release at early and late time periods after the end of OGD insult and that Na^+-dependent GluT-inhibitor DL-TBOA treatment reduced its release. Excess glutamate activates iGluR causing iGluR-mediated excitotoxicity, a crucial mediator of the damage developing WM (Follett et al., 2004). Glutamate excitotoxicity leading to degeneration of motor neurons, mitochondrial dysfunction, oxidative stress, inflammation and apoptosis (Corona et al., 2007). Blocking AMPA/kainate receptors alone during ischemia did not preserves axon potentials in myelinated optic nerve, and a similar lack of improvement was observed when NMDA GluRs were blocked alone (Bakiri et al., 2008). Our findings suggest that that inhibition of AMPA, kainate, and NMDA iGluRs together is more protective against consequences of ischemic insult, suggesting that clinical application of NMDA GluR antagonists to treat developing WMI would require companioning it with AMPA/kainate antagonists.

The occurrence of ischemic episode is unpredictable, often making pre-treatment not feasible. The efficiency of iGluR blockers as a post-treatment strategy for developing WM ischemia, however, is still unclear. In the present study, we found that post-treatment with combined iGluR block (MK-801+NBQX) to a time point shortly (20 min) after WMI resulted in a significant decrease in WM damage, suggesting persistent activation of iGluR signaling by extracellular glutamate after the end of OGD-insult. The findings described above demonstrate that although pre-treatment with MK-801+NBQX before ischemic insult was the most effective, the consistent protection conferred by post-injury treatment with combined iGluR block suggests a window of opportunity to attenuate WMI at birth. Because ischemic episodes are often associated with premature infants and these infants are generally maintained in a constantly monitored neonatal intensive care unit, commencing treatment even within few minutes' post-insults is feasible.

One key question about WMI is the route by which cell death is triggered, and accordingly, which of signaling pathways could be chosen as a therapeutic target. The expression of anti-apoptotic gene BCL-2 and neurotrophin BDNF are implicated in the cell death regulation (Hardingham et al., 2002; Hwang and Chun, 2012). For example, BCL-2 plays a crucial role in the cell death control through the stabilization of the mitochondrial membrane potential., thereby preventing release of cytochrome c and APAF-1 in the cytosol, which recruits pro-apoptotic pathways (Shimizu et al., 1999; Andrabi et al., 2019). In the present study, we found that WMI led to upregulation of caspase-8, -1, -9, and -3 expression compared to SHAM group, and that treatment with MK-801+NBQX post-WMI modulated their expression. This suggests that reducing caspase expression may be a mechanism by which combined iGluR block confers protection against ischemia induced WMI.

The WM elements are separately under ischemic attack. Overactivation of iGluRs plays a crucial role in mediating Ca^{2+}-dependent injury of OL populations and myelin with a subsequent axonal degeneration (Salter and Fern, 2005; Stys and Lipton, 2007). Given that presence of AMPA, kainate, and NMDA iGluRs on all WM compartments (Dohare et al., 2016; Fern and Matute, 2019; Salter and Fern, 2005; Stys and Lipton, 2007), we, however, investigated whether the inhibition of iGluR would attenuate WM elements in our *ex vivo* model and OL cultures (Deng, 2010), as well as in acute tissue cultures (Salter and Fern, 2005). A study using rat optic nerve to model WMI, to study the early OGD effects found that iGluR blockers were effective against acute ischemic injury to OL populations (Salter and Fern, 2005). These blockers were also effective when examined 24 h after ischemia induced injury to neurons in hippocampus OSCs (Pringle et al., 1997). In a rat model of PVL, blockers of iGluRs were also effective in attenuating WMI. Using an *ex vivo* model of WMI, we found that post-treatment with MK-801+NBQX significantly mitigates OL loss, a consequence of WM ischemia and

ischemia related CNS disorders seen in premature infants. Gene and protein expression studies demonstrate that combined iGluR inhibition with MK-801+NBQX protected myelin profile and transcription factors that regulating OL development and remyelination when administrated after OGD insult.

Remyelination after injury-induced demyelination is thought to depend – at least in part – on the OPC recruitment (Rivers et al., 2008; Li et al., 2015). *Ex vivo* brain models have been repeatedly employed to study remyelination after injury induced demyelination (Birgbauer et al., 2004; Harrer et al., 2009). Prior studies (Harrer et al., 2009; Yang et al., 2011) showed that OPCs can proliferate and then differentiate into mature forms within 3 days in brain slice system. In the present study, we found that MK-801+NBQX treatment protected mitotic behavior of $NG2^+$ OPCs in response to WMI. This observation raises the question whether it also enhances OPC differentiation after WMI induces demyelination. Using BrdU immunostaining, we found that treatment with combined iGluR block after injury enhanced $NG2^+$ OPC differentiation into MBP^+ OLs. The fact that iGluR blockers preserved OPC mitotic behavior, increased the number of new OLs ($BrdU^+/MBP^+$ OLs), and increased percentage of MBP^+ membranes on NF^+ axons in this model, supports our idea that the iGluR inhibition may impose a milieu favoring OPC recruitment and differentiation.

Another major finding in this study is how inflammatory response contributes to the deleterious impacts of ischemic insult on WM elements, including OL death and myelin disruption in the context of WMI. OL destruction resulting in demyelination is a central feature of a number of human demyelinating disorders, including multiple sclerosis and cerebral palsy (Compston and Coles, 2008). In demyelinating diseases, there are many overlapping cell death mechanisms of OLs. Myelination disturbances can occur due to apoptotic cascade activation induced by cytokines or due to their susceptibility to excitotoxicity. Microglia and astrocyte recruitment is a hallmark of the inflammatory response to hypoxia-ischemia (Deng, 2010; Murugan et al., 2011). After injury, microglia and astrocyte activation is accompanied by the releasing of massive proinflammatory mediators including reactive oxygen species (ROS) and cytokines (Deng et al., 2008; Murugan et al., 2011). Importantly, microglia express iGluR receptors; and activation of their iGluRs triggers release of TNF-α and IL-1β in conditions of brain injury (Noda et al., 2000; Takahashi et al., 2003; Kong et al., 2019). Additionally, astrocytes after injury were noted to increase release of pro-inflammatory cytokines, such as TNF-α and IL-6 as well as intercellular iNOS, NO, and ROS (Zhang et al., 2018). Production of ROS triggers inflammation and apoptosis (Dirnagl et al., 1999; Khatri et al., 2018). Evidence indicates that cytokines (e.g., TNF-α and IL-1β), ROS (e.g., NO), and iNOS are toxic to OL lineage cells and myelin and interfere with OPC proliferation (Deng et al., 2008; Murugan et al., 2011; Wu et al., 2010; Yu et al., 2020).

Cytokines (TNF-α and IL-1β) injures OLs and delays myelination through binding to their respective receptors on the OLs (Deng et al., 2008). OL loss and demyelination are also thought to result from collateral damage from iNOS in microglia (Yu et al., 2020) *via* NO production (Murugan et al., 2011). ROS, such as NO can react with superoxide anions to form peroxynitrite that can oxidize essential molecules such as DNA, leading to cellular damage (Zhou et al., 2019). In this study, we found that ischemia induced an exaggerated release of glutamate which causes WMI. Binding of glutamate to its receptors can promote a further elevation in Ca^{2+} entry (Matute, 2011). Indeed Ca^{2+} overload upon activation of these receptors can activate multiple putative damaging proteins, such as iNOS. NMDA-inhibitor MK-801 alone was previously reported to downregulate ischaemia induced iNOS, NO, and cytokine production (Murugan et al., 2011; Park et al., 2016). In the present study, we found that combined iGluR block upon WMI suppressed inflammation. Specifically, we found that combined iGluR block decreased apoptosis among OPCs and releasing of cytokines and iNOS. Collectively, these findings could in fact suggest that iGluR activation contributed to OL death and upregulated cytokine and iNOS expression; and MK-801+NBQX treatment seemingly alleviated inflammation, decreased cytokine and iNOS, and consequently preserved OPC survival., proliferation, and maturation.

CONCLUSION

In conclusion, we highlight the potential therapeutic values of iGluR inhibition in specifically in perverting or reversing ischemic WM pathology associated with a number of many neurological deficits. Additionally, our findings reinforce the linkage between inflammation and demyelination. The occurrence of ischemic episode is unpredictable, making pre-treatment not possible. The efficiency and effectiveness of combined iGluR block MK-801+NBQX as a post-treatment strategy for developing WM ischemia, however, is still unclear. The findings of this study showed that delaying treatment with combined iGluR block to a time point shortly (20 min) after ischemia preserved WM elements, suggesting persistent of iGluR signaling by extracellular glutamate after the end of ischemic-insult. Because newborn infants are generally maintained in a con-

stantly monitored neonatal intensive care unit, iGluR inhibition even within few minutes' post-insults is feasible to at least minimize WM damage.

ACKNOWLEDGEMENTS

The execution of this experiment was supported by the University of Tripoli, Libya.

REFERENCES

Al-Griw MA, Alghazeer RO, Awayn,A, Shamlan G, Eskandrani AA, Alnajeebi AM, Babteen NA, Alansari WS (2021) Selective adenosine A2A receptor inhibitor SCH58261 reduces oligodendrocyte loss upon brain injury in young rats. Saudi Journal Biol Sciences 28: 310–316.

Andrabi SS, Ali M, Tabassum H, Parveen S, Parvez S (2019) Pramipexole prevents ischemic cell death via mitochondrial pathways in ischemic stroke. Dis Model Mech 12: dmm033860.

Arai K, Lo E (2009) Experimental models for analysis of oligodendrocyte pathophysiology in stroke. Exp Translational Stroke Medicine 1: 1–6.

Back SA, Han BH, Luo NL, Chricton CA, Xanthoudakis S, Tam J, Arvin, KL, Holtzman, DM (2002) Selective vulnerability of late oligodendrocyte progenitors to hypoxia-ischemia. J Neurosci 22: 455–463.

Back SA, Rosenberg PA (2014) Pathophysiology of glia in perinatal white matter injury. Glia 62, 1790–1815.

Bakiri Y, Hamilton NB, Káradóttir R, Attwell D (2008) Testing NMDA receptor block as a therapeutic strategy for reducing ischaemic damage to CNS white matter. Glia 56: 233–240.

Baltan S, Murphy SP, Danilov CA, Bachleda A, Morrison RS (2011) Histone deacetylase inhibitors preserve white matter structure and function during ischemia by conserving ATP and reducing excitotoxicity. J Neurosci 31: 3990–3999.

Beppu, K, Sasaki, T, Tanaka, KF, Yamanaka, A, Fukazawa, Y, Shigemoto, R, Matsui, K (2014) Optogenetic countering of glial acidosis suppresses glial glutamate release and ischemic brain damage. Neuron 81: 314–320.

Birgbauer E, Rao TS, Webb M (2004) Lysolecithin induces demyelination in vitro in a cerebellar slice culture system. J Neurosci Res 78: 157–166.

Butt AM, Fern RF, Matute C (2014) Neurotransmitter signaling in white matter. Glia 62: 1762–1779.

Butt AM, Ransom BR (1993) Morphology of astrocytes and oligodendrocytes during development in the intact rat optic nerve. Journal Comparative Neurol 338: 141–158.

Canedo-Antelo M, Serrano MP, Manterola A, Ruiz A, Llavero F, Mato S, Zugaza JL, Pérez-Cerdá F, Matute C, Sánchez-Gómez MV (2018) Inhibition of casein kinase 2 protects oligodendrocytes from excitotoxicity by attenuating JNK/p53 signaling cascade. Front Mol Neurosci 13: 333.

Cohen GM (1997) Caspases: the executioners of apoptosis. Biochemistry Journal 326, 1–16.

Compston A, Coles A (2008) Multiple sclerosis. Lancet 372: 1502–1517.

Corona JC, Tovar-y-Romo LB, Tapia R (2007) Glutamate excitotoxicity and therapeutic targets for amyotrophic lateral sclerosis. Expert Opin Ther Targets 11: 1415–1428.

Deng W (2010) Neurobiology of injury to the developing brain. Nature Rev| Neurosci 6: 328–336.

Deng Y, Lu J, Sivakumar V, Ling E, Kaur C (2008) Amoeboid microglia in the periventricular white matter induce oligodendrocyte damage through expression of proinflammatory cytokines via MAP kinase signaling pathway in hypoxic neonatal rats. Brain Pathol 1: 387–400.

Dirnagl U, Iadecola C, Moskowitz MA (1999) Pathobiology of ischaemic stroke: an integrated view. Trends Neurosci 22: 391–397.

Dohare P, Zia MT, Ahmed E, Ahmed A, Yadala V, Schober AL, Ortega JA, Kayton R, Ungvari Z, Mongin AA, et al. (2016) AMPA-kainate receptor inhibition promotes neurologic recovery in premature rabbits with intraventricular hemorrhage. J Neurosci 16: 3363–3377.

Doyle S, Hansen DB, Vella J, Bond P, Harper G, Zammit C, Valentino M, Fern R (2018) Vesicular glutamate release from central axons contributes to myelin damage. Nat Commun 12: 1032.

Evonuk KS, Doyle RE, Moseley CE, Thornell IM, Adler K, Bingaman AM, Bevensee MO, Weaver CT, Min B, DeSilva TM (2020) Reduction of AMPA receptor activity on mature oligodendrocytes attenuates loss of myelinated axons in autoimmune neuroinflammation. Sci Adv 8: eaax5936.

Fancy SP, Chan JR, Baranzini SE, Franklin RJ, Rowitch DH (2011) Myelin regeneration: a recapitulation of development? Ann Rev Neurosci 34: 21–43.

Fancy SP, Zhao C, Franklin RJ (2004) Increased expression of Nkx2.2 and Olig2 identifies reactive oligodendrocyte progenitor cells responding to demyelination in the adult CNS. Mol Cell Neurosci 27: 247–254.

Fern R, Matute C (2019) Glutamate Receptors and White Matter Stroke. Neurosci Lett 694: 86–92.

Follett PL, Deng W, Dai W, Talos DM, Massillon LJ, Rosenberg PA, Volpe JJ, Jensen FE (2004) Glutamate receptor-mediated oligodendrocyte toxicity in periventricular leukomalacia: a protective role for topiramate. J Neurosci 24: 4412–4420.

Fu H, Qi Y, Tan M, Cai J, Takebayashi H, Nakafuku M, Richardson W, Qiu M (2002) Dual origin of spinal oligodendrocyte progenitors and evidence for the cooperative role of Olig2 and Nkx2.2 in the control of oligodendrocyte differentiation. Development 129: 681–693.

Hardingham GE, Fukunaga Y, Bading H (2002) Extrasynaptic NMDARs oppose synaptic NMDARs by triggering CREB shut-off and cell death pathways. Nature Neurosci 5: 405–414.

Harrer MD, von Büdingen HC, Stoppini L, Alliod C, Pouly S, Fischer K, Goebels N (2009) Live imaging of remyelination after antibody-mediated demyelination in an ex-vivo model for immune mediated CNS damage. Exp Neurol 216: 431–438.

Hwang CK, Chun HS (2012) Isoliquiritigenin isolated from licorice Glycyrrhiza uralensis prevents 6-hydroxydopamine-induced apoptosis in dopaminergic neurons. Biosci Biotechnol Biochem 76: 536–543.

Jensen FE (2005) Role of glutamate receptors in periventricular leukomalacia. J Child Neurol 20: 950–959.

Khatri N, Thakur M, Pareek V, Kumar S, Sharma S, Datusalia AK (2018) Oxidative stress: major threat in traumatic brain injury. CNS Neurol Disord Drug Targets 17: 689–695.

Kong X, Zhang Z, Fu T, Ji J, Yang J, Gu Z (2019) TNF-α regulates microglial activation via the NF-κB signaling pathway in systemic lupus erythematosus with depression. Int J Biol Macromol 125: 892–900.

Levine,JM, Card JP (1987) Light and electron microscopic localization of a cell surface antigen (NG2) in the rat cerebellum: association with smooth protoplasmic astrocytes. J Neurosci 7: 271 I-2720.

Li Y, Tang G, Liu Y, He X, Huang J, Lin X, Zhang Z, Yang G, Wang Y (2015) CXCL12 gene therapy ameliorates ischemia-induced white matter injury in mouse brain. Stem Cells Transl Med 2: 1122–1130.

Mangin JM, Li P, Scafidi J, Gallo V (2012) Experience-dependent regulation of ng2 progenitors in the developing barrel cortex. Nat Neurosci 15: 1192–1194.

Matute C (2011) Glutamate and ATP signalling in white matter pathology. J Anat 219: 53–64.

Matute C, Domercq M, Sanchez-Gomez M (2006) Glutamate-mediated glial injury: mechanisms and clinical importance. Glia 53: 212–224.

McTigue DM, Wei P, Stokes BT (2001) Proliferation of NG2-positive cells and altered oligodendrocyte numbers in the contused rat spinal cord. J Neurosci 21: 3392–3400.

Murugan M, Sivakumar V, Lu J, Ling EA, Kaur C (2011) Expression of N-methyl D-aspartate receptor subunits in amoeboid microglia mediates production of nitric oxide via NF-kB signaling pathway and oligodendrocyte cell death in hypoxic postnatal rats. Glia 59: 521–539.

Nicholson DW, Ali A, Thornberry NA, Vaillancourt JP, Ding CK, Gallant M, Gareau Y, Griffin P, Labelle M, Lazebnik YA, et al. (1995) Identification and inhibition of the ICE/CED-3 protease necessary for mammalian apoptosis. Nature 376: 37–43.

Noda M, Nakanishi H, Nabekura J, Akaike N (2000) AMPA-kainate subtypes of glutamate receptor in rat cerebral microglia. J Neuroscience 20: 251–258.

Ogawa S, Hagiwara M, Misumi S, Tajiri N, Shimizu T, Ishida A, Suzumori N, Sugiura-Ogasawara M, Hida H (2020) Transplanted oligodendrocyte progenitor cells survive in the brain of a rat neonatal white matter injury model but less mature in comparison with the normal brain. Cell Transplant 29: 963689720946092.

Olivier P, Fontaine RH, Loron G, Van-Steenwinckel J, Biran V, Massonneau V, Kaindl A, Dalous J, Charriaut-Marlangue C, Aigrot M., et al. (2009) Melatonin promotes oligodendroglial maturation of injured white matter in neonatal rats. PLoS ONE 4: e7128.

Park T, Chen,H, Kevala K, Lee JW, Kim HY (2016) N-Docosahexaenoylethanolamine ameliorates LPS-induced neuroinflammation via cAMP/PKA-dependent signaling. J Neuroinflammation 13: 284.

Pringle AK, Iannotti F, Wilde GJ, Chad JE, Seeley PJ, Sundstrom LE (1997) Neuroprotection by both NMDA and non-NMDA receptor antagonists in in vitro ischemia. Brain Research 755: 36–46.

Rivers LE, Young KM, Rizzi M, Jamen F, Psachoulia K, Wade A, Kessaris N, Richardson WD (2008) PDGFRA/NG2 glia generate myelinating oligodendrocytes and piriform projection neurons in adult mice. Nature Neuroscience 11: 1392–1401.

Salter MG, Fern R (2005) NMDA receptors are expressed in developing oligodendrocyte processes and mediate injury. Nature 438: 1167–1171.

Sanchez-Gomez MV, Alberdi E, Ibarretxe G, Torre I, Matute C (2003) Caspase-dependent and caspase-independent oligodendrocyte death mediated by AMPA and kainate receptors. J Neurosci 23: 9519–9528.

Sanchez-Gomez MV, Alberdi E, Perez-Navarro E, Alberch J, Matute C (2011) Bax and calpain mediate excitotoxic oligodendrocyte death induced by activation of both AMPA and kainate receptors. J Neurosci 31: 2996–3006.

Shimizu S, Narita M, Tsujimoto Y (1999) Bcl-2 family proteins regulate the release of apoptogenic cytochrome c by the mitochondrial channel VDAC. Nature 399: 483–487.

Stirling DP, Stys PK (2010) Mechanisms of axonal injury: internodal nanocomplexes and calcium deregulation. Trends Mol Med 16: 160–170.

Stoppini,L, Buchs PA, Muller D (1991) A simple method for organotypic cultures of nervous tissue. J Neurosci Methods 37: 173–182.

Stys PK, Lipton SA (2007) White matter NMDA receptors: an unexpected new therapeutic target? Trends Pharmacol Sci 28: 561–566.

Suyama K, Watanabe M, Sakai D, Osada T, Imai M, Mochida J (2007) Nkx2.2 expression in differentiation of oligodendrocyte precursor cells and inhibitory factors for differentiation of oligodendrocytes after traumatic spinal cord injury. J Neurotrauma 24: 1013–1025.

Takahashi JL, Giuliani F, Power C, Imai Y, Yong VW (2003) Interleukin-1beta promotes oligodendrocyte death through glutamate excitotoxicity. Ann Neurol 53: 588–595.

Volpe JJ (2009) Brain injury in premature infants: a complex amalgam of destructive and developmental disturbances. Lancet Neurol 8: 110–124.

Wu J, Yoo S, Wilcock D, Lytle JM, Leung PY, Colton CA, Wrathall JR (2010) Action of NG2(+) glial progenitors and microglia/macrophages from the injured spinal cord. Glia 58: 410–422.

Yang Y, Lewis R, Miller RH (2011) Interactions between oligodendrocyte precursors control the onset of CNS myelination. Develop Biol 350: 127–138.

Yu Y, Luo X, Li C, Ding F, Wang M, Xie M, Yu Z, Ransom BR, Wang W (2020) Microglial Hv1 proton channels promote white matter injuries after chronic hypoperfusion in mice. J Neurochem 152: 350–367.

Zhang F, Zhang J, Yang W, Xu P, Xiao Y, Zhang H (2018) 6-gingerol attenuates lps-induced neuroinflammation and cognitive impairment partially via suppressing astrocyte overactivation. Biomed Pharnacother 107: 1523–1529.

Zhou X, Ding X, Shen J, Yang D, Hudson LG, Liu KJ (2019) Peroxynitrite contributes to arsenic-induced PARP-1 inhibition through ROS/RNS generation. Toxicol Appl Pharmacol 378: 114602.